Beurteilung der Überlastbarkeit von Windparktransformatoren durch Monitoring

N. Schmidt
Universität Stuttgart
nicolas.schmidt@ieh.uni-stuttgart.de, Germany

J. Wildenhain
EWE NETZ GmbH
jens.wildenhain@ewe.de
Germany

R. Skrzypek
ALSTOM Grid
raimund.skrzypek@alstom.com
Germany

KURZFASSUNG

Dieser Beitrag beschreibt einen Ansatz, mit dem die Fähigkeit zur Überlast bei ölgekühlten Transformatoren in Abhängigkeit von der Umgebungstemperatur bestimmt werden kann. Hierfür wurde ein vereinfachendes, empirisch gestütztes Modell entwickelt, welches Veränderungen der Öltemperatur mit hoher Genauigkeit prognostizieren kann. Entsprechend den Vorstellungen des sogenannten *Einkörpermodells* wird darin der gesamte Transformator als ein homogen temperierter Körper mit einer bestimmten Wärmekapazität betrachtet. Zudem werden alle elektrischen Verluste als die Summe der lastabhängigen Verluste und Leerlaufverluste angesetzt und als Eintrag gleichmäßig verteilter Wärme berücksichtigt. Im Gegensatz zu früheren Ansätzen wird der Wärmeaustausch mit der Umgebung über eine komplexe Funktion abgebildet, die in erster Linie von der Temperaturdifferenz zwischen dem Transformator und der Umgebung abhängt. Darüber hinaus werden zeitabhängige Größen, wie beispielsweise die anliegende Last, das vorliegende Temperaturniveau sowie die zugehörigen Temperaturgradienten neben temperaturabhängigen Materialeigenschaften als Einflussfaktoren für die Bestimmung des Wärmeaustauschs berücksichtigt.

Um das Verhalten eines bestimmten Transformators modellieren zu können, werden im vorgestellten Modell mehrere empirische Faktoren verwendet. Für deren Bestimmung hat sich ein repräsentativer Betriebszeitraum über zwei bis vier Wochen eines zu untersuchenden Transformators bereits als ausreichend erwiesen. Um das entwickelte Modell validieren und dessen Zuverlässigkeit untersuchen zu können, wurden Messdaten von mehreren ONAN-und ONAF-Transformatoren herangezogen. Die zugehörigen Datensätze umfassen die Öl- und Umgebungstemperatur, sowie die anliegende Last und den Zustand der Kühlanlage. Darüber hinaus wurden die Daten der entsprechenden Typenschilder integriert. Im Anschluss an die Berechnung der Öltemperatur, wird die maximale Belastbarkeit bestimmt, welche auch bei dauerhafter Beanspruchung in einer Hot-Spot-Temperatur unterhalb kritischen Niveaus resultiert. Hierfür wurde auf die IEC 60076-7 [1] zurückgegriffen. Auf Basis der gewonnen Ergebnisse konnte schließlich für jeden untersuchten Transformator eine charakteristische lineare Funktion abgeleitet werden, welche die maximale Überlastbarkeit in Abhängigkeit der Umgebungstemperatur angibt. Im Fall der untersuchten ONAN- und ONAF-Transformatoren der Leistungsklasse zwischen 31,5 und 63 MVA zeigten sich erhebliche Überlastungspotenziale.

1 INTRODUCTION

The integration of renewable energy technologies into present power grids implicates significant challenges for the network operators. Due to its unsteady character, the commonly provided output of a wind park often results in peak loading of the connected network components. Furthermore, the ongoing extension of established wind farms and the assembly of new wind parks amplify the emerging peak loads for the existent technical resources. This development might induce network operators to tolerate temporary loading levels beyond name plate rating. Nevertheless, long term consequences concerning the ageing of the equipment have to be taken into account.
The lifetime performance of a power transformer strongly depends on the temperatures its materials have been exposed to. Because of their significant effect, a profound knowledge about these temperatures is of great interest. While a current state may also be derived from measurements, prospective developments can only be obtained by modelling. Due to transient load conditions, changing ambient conditions, adjustable cooling systems and their design and operation principles, transformers represent a rather complex thermal system. In addition, the particular design of a certain transformer, with its applied materials and installed components, complicates precise simulations tremendously. However, knowledge about the exact temperature distribution inside a transformer may not be necessary within the scope of every desired application. For instance, the determination of a constant, non-critical level of overload might already be achieved by means of a simplified thermal model.

2 THERMAL TRANSFORMER MODEL

The applied thermal model bases upon the idea of an one-body-model (**Figure 1**). Consequently, the entire transformer is considered as a single, homogenous tempered body with the thermal capacity C_{th}. All electrical losses P_{loss} are perceived as an input of the equally distributed heat $\dot{Q}_{in}$ and assumed to be the sum of the load losses P_{sc} and the no-load losses P_0, as stated in equation (1). For the nominal load losses $P_{sc,n}$, the middle position of the on-load tap-changer is applied. The time-dependent load factor $k(t)$ is thereby determined by the ratio of the actual current $I(t)$ to the nominal current I_n.

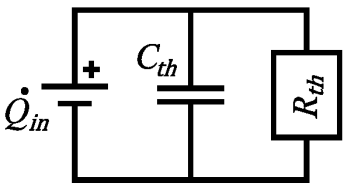

Figure 1: One-body-model

$$\dot{Q}_{in}(t) = P_{loss} = P_0 + k(t)^2 \cdot P_{sc,n} \quad \text{with} \quad k(t) = \frac{I(t)}{I_n} \tag{1}$$

The heat flow rate $\dot{Q}_{out}$ coming out of the transformer's cooling system is assumed to be proportional to the reciprocal value of the thermal resistance R_{th} and to the temperature gradient of the top-oil temperature ϑ_{TO} and the ambient temperature ϑ_{amb}. This concludes in

$$\dot{Q}_{out}(t) = \frac{1}{R_{th}(t)} \cdot \left(\vartheta_{TO}(t) - \vartheta_{amb}(t)\right) \quad \text{with} \quad R_{th}(t) = \frac{1}{\alpha(t) \cdot A} \; . \tag{2}$$

While A describes the heat transferring surface, α represents the corresponding heat transfer coefficient. The energy balance finally factors in the thermal capacity C_{th}, resulting in

$$P_{loss}(t) - \dot{Q}_{out}(t) = C_{th} \cdot \dot{\vartheta}_{TO}(t) \quad \text{with} \quad C_{th} = \sum m_i \cdot c_i \; . \tag{3}$$

Equation (3) shows, that the thermal inertia of the transformer is modelled proportional to the changing rate of the top-oil temperature. The total thermal capacity C_{th} of the modelled transformer is calculated from the sum of all considered thermal masses (tank, windings, core and oil) multiplied with each corresponding specific thermal capacity.

Combining equation (2) and (3) leads to

$$P_{loss}(t) - \frac{1}{R_{th}(t)} \cdot \left(\vartheta_{TO}(t) - \vartheta_{amb}(t)\right) = C_{th} \cdot \dot{\vartheta}_{TO}(t) \quad . \tag{4}$$

Solving the differential equation (4) provides an approximation for the temperature change along the time step from t to $t+\Delta t$ in the form of

$$\Delta\vartheta_{TO,t\to t+\Delta t} = \left(\bar{P}_{loss}(t) \cdot \bar{R}_{th}(t) + \bar{\vartheta}_{amb}(t) - \vartheta_{TO}(t)\right) \cdot \left(1 - e^{\frac{-\Delta t}{\bar{R}_{th}(t) \cdot C_{th}}}\right) \quad . \tag{5}$$

All properties in equation (5) carrying a bar refer to the averaged value of the corresponding property during the time step from t to $t+\Delta t$. The only remaining unknown in this equation is the thermal resistance R_{th}, that can be either taken out of standards or be determined empirically by a set measurements.

Instead of assessing R_{th} by a constant value as in earlier investigations [2], a more complex approach was chosen. **Figure 2** displays the underlying principle, that was applied to model the physical conditions of the heat exchange between the transformer and its surroundings. It subdivides the thermal resistance into three parts, representing different principles and locations of heat transfer. Although the thermal model, according to equation (5), takes only one temperature for the entire transformer into account (ϑ_{TO}), Figure 2 also refers to the temperature of the windings ϑ_{wdg}. This necessitates a transformation that will be described in detail below (see equation (8)). To model the transport of heat from the locations of heat generation to the ambience, in a first step $R_{conv,wdg\text{-}TO}$ takes the heat convection between the windings and the oil into account. Subsequently, $R_{rad,TO\text{-}amb}$ includes the heat transfer between the tank and the ambience due to heat radiation. Finally, $R_{conv,TO\text{-}amb}$ factors in the heat convection between the transformer's radiators and the ambience. Neglecting the thermal resistance of the convecting oil at the heat transferring surfaces of the tank as well as at the radiators results in identical temperatures of the oil, the tank and the radiators. According to the calculation rules for thermal resistances , the overall thermal resistance $R_{th,total}$ then can be calculated with

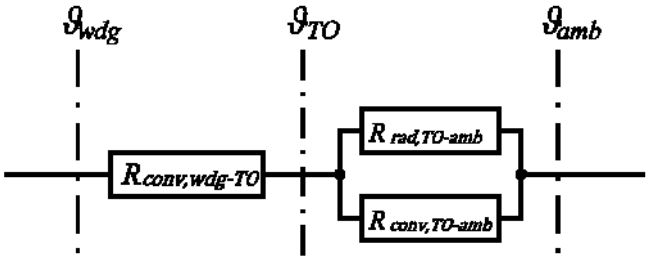

Figure 2: R_{th}-Modelling

$$R_{th,total} = R_{conv,wdg-TO} + \frac{1}{\frac{1}{R_{rad,TO-amb}} + \frac{1}{R_{conv,TO-amb}}} \quad , \tag{6}$$

or with $R_i = {}^{1}/_{(\alpha \cdot A)_i}$

$$R_{th,total} = \frac{1}{(A \cdot \alpha)_{conv,wdg-TO}} + \frac{1}{(A \cdot \alpha)_{rad,TO-amb} + (A \cdot \alpha)_{conv,TO-amb}} \quad . \tag{7}$$

However, the corresponding heat flow rate of $R_{th,total}$ would refer to the temperature gradient $\Delta\vartheta_{wdg-amb}$. To avoid a contradiction with the equations (1)-(5), $R_{th,total}$ is transformed to

$$R_{th} = R_{th,total} \cdot \frac{\Delta\vartheta_{TO-amb}}{\Delta\vartheta_{wdg-amb}} \quad (8)$$

Beside the heat transfer coefficients α_i and the corresponding areas of heat transfer A_i , also the applied winding temperature ϑ_{wdg} has to be modelled appropriately. The latter is accomplished by

$$\vartheta_{wdg}(t) = \vartheta_{TO}(t) + x_{g1} \cdot (k(t)^2)^{x_{g2}} \quad (9)$$

with the empirical factors x_{g1} and x_{g2} . Equation (9) therefore assumes that the temperature gradient between oil and windings depends on the loading rate $k(t)$. To model the heat transferring areas, additional empirical factors have to be applied. It would be possible to apply three empirical factors for three unknown values directly, nevertheless the presented results rely on correlations displayed in equation (10). This offers the opportunity to keep the resulting values of the empirical factors within reasonable boundaries with respect to their physical equivalent. The factor x_h refers to the geometrical height of the winding while x_U resembles the sum of all wetted perimeters formed by the vertical cooling channels inside the windings. Finally, x_p can be interpreted as the number of applied radiator plates.

$$A_{conv,wdg-TO} = x_U \cdot x_h \; ; \; A_{conv,TO-amb} = x_p \cdot 4 \cdot x_h^2 \; ; \; A_{rad,TO-amb} = 10 \cdot x_h^2 \quad (10)$$

The purpose of the roughly estimated constant values in equation (10) is to couple the empirical factors within the calculation of the heat transferring surfaces in a physical reasonable manner without introducing new empirical factors. Nevertheless, values differing from the chosen ones might very well lead to similar simulation results. The heat transfer coefficients for the natural convection of oil inside the windings $\alpha_{nc,wdg\text{-}TO}$ and air inside the radiator panels $\alpha_{nc,TO\text{-}amb}$ are modelled on basis of correlations given by the VDI Heat Atlas [3]. In case of oil, a scenario of a vertical annular gap with the characteristic height of x_h and a gap width of x_d is chosen. A scenario of vertical sets of plates with a characteristic height of x_h and a plate distance of $5 \cdot x_d$ is selected for the natural convection of air. As mentioned before, a value differing from the roughly estimated value of 5 might very well lead to similar simulation results. Furthermore, temperature dependent material properties for oil and air are applied. To cover forced convection (e.g. for ONAF or OFAF cooling systems), a linear extension depending on the number of active fans/ pumps $n_{fan/pump}$ is applied. With the additional empirical factors $x_{fc,i}$ follows

$$\alpha_{conv,i} = \alpha_{nc,i} + n_{fan/pump} \cdot x_{fc,i} \quad (11)$$

As a possible future development, instead of this strongly simplifying approach, elaborated functions or correlations for forced convection could be applied alternatively. Finally, the heat transfer coefficient of the heat radiation is given by

$$\alpha_{rad,TO-amb} = \frac{\varepsilon \cdot \sigma \cdot (T_{TO}^4 - T_{amb}^4)}{\Delta\vartheta_{TO-amb}} \quad (12)$$

with an approximated emission coefficient $\varepsilon = 0{,}9$ and the Stefan-Boltzmann constant σ. In summary, the presented model pursuits the goal to cover the basic thermal kinetics of a transformer sufficiently. To make it as applicable as possible, the amount of required information is kept as little as possible. Consequently, since the introduced model depends on additional specifications and data, the lack of information is covered empirically. To validate the capabilities of this approach, the following sections will present modelling results that could be gathered applying the presented thermal model.

3 MODELLING RESULTS

To point out the advantage of a variably modelled thermal resistance in comparison to a constant thermal resistance, **Figure 3** shows the corresponding modelling results for a 31.5 MVA ONAN transformer. In case of a constant thermal resistance, the top-oil temperature is overestimated in periods with a high loading rate while in times with a low loading rate the top-oil temperature is underestimated. In comparison, the presented thermal model covers both loading states very well. The consulted evaluation period to determine the empirical parameters was thereby set to one week.

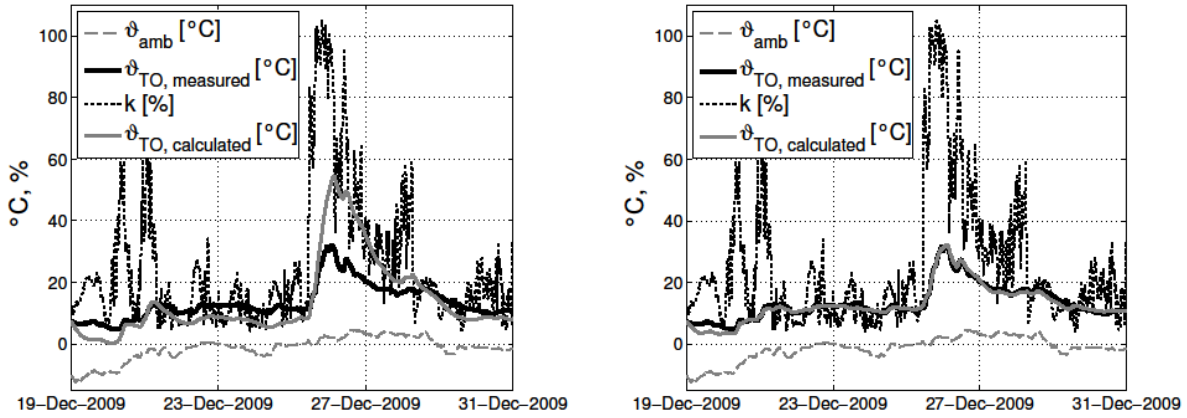

(a) R_{th} = const. (b) $R_{th} = R_{th,model}$

Figure 3: Modelling results for a 31.5 MVA ONAN transformer

Figure 4 shows the influence of the evaluation period on the modelling results for a 40 MVA ONAF transformer. It can be seen that an evaluation period of four weeks is already sufficient to achieve expedient results. Accordingly, a longer evaluation period provides only little improvement.

4 ASSESSMENT OF OVERLOAD CAPABILITIES

The loading guide for oil-immersed power transformers IEC 60076-7 [1] provides an equation to determine the resulting hot-spot temperature ϑ_{HS} at a given constant loading rate k depending on the emerging temperature gradient between the top-oil temperature and the ambient temperature at nominal conditions $\Delta\vartheta_{TO\text{-}amb,n}$. It states

$$\vartheta_{HS} = \vartheta_{amb} + \Delta\vartheta_{TO-amb,n} \cdot \left[\frac{1 + \frac{P_{SCn}}{P_0} \cdot k^2}{1 + \frac{P_{SCn}}{P_0}}\right]^x + H \cdot g_r \cdot k^y \quad , \tag{1}$$

with the hot-spot factor H, the averaged temperature gradient between the windings and the oil g_r, the oil-exponent x and the winding-exponent y. Equation (4) delivers at constant conditions $\Delta\vartheta_{TO-amb,n} = P_{loss,n} \cdot R_{th} = (P_0 + P_{SCn}) \cdot R_{th}$. Applied in equation (1) follows

$$\vartheta_{HS} = \vartheta_{amb} + P_{loss,n} \cdot R_{th} \cdot \left[\frac{P_{loss}(k)}{P_{loss}}\right]^x + H \cdot g_r \cdot k^y \quad . \tag{2}$$

In case of ONAN- and ONAF-transformers, IEC 60076-7 [1] provides a set of possible values for the introduced factors with $x = 0.8$, $y = 1.3$, $H = 1.3$ and $g_r = 20$ K. Moreover, it recommends a hot-spot temperature of $\vartheta_{HS} = 98$ °C to maintain a nominal aging rate. Consequently, applying the validated

thermal resistance of a certain transformer can permit the determination of a maximum, non-critical loading rate k_{max} that results in a nominal aging rate. **Figure 5** displays the results of the described proceeding for the investigated transformers approximated with linear functions in the form of

$$k_{max} = a \cdot \vartheta_{amb} + b \ . \quad (3)$$

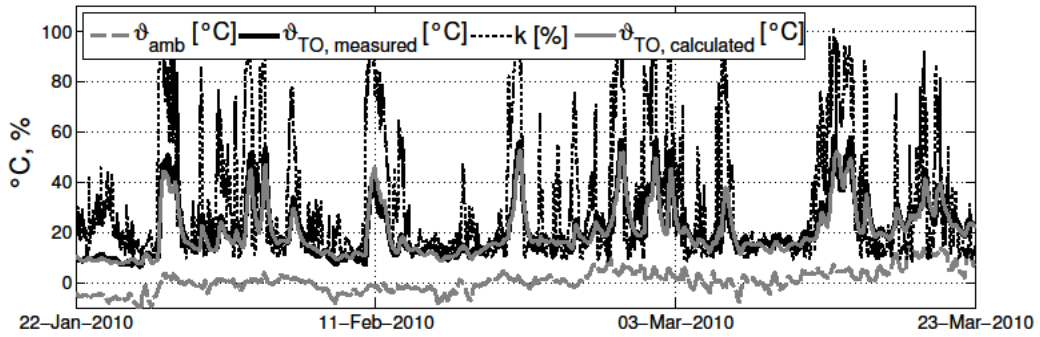

(a) Empirical evaluation time of four weeks

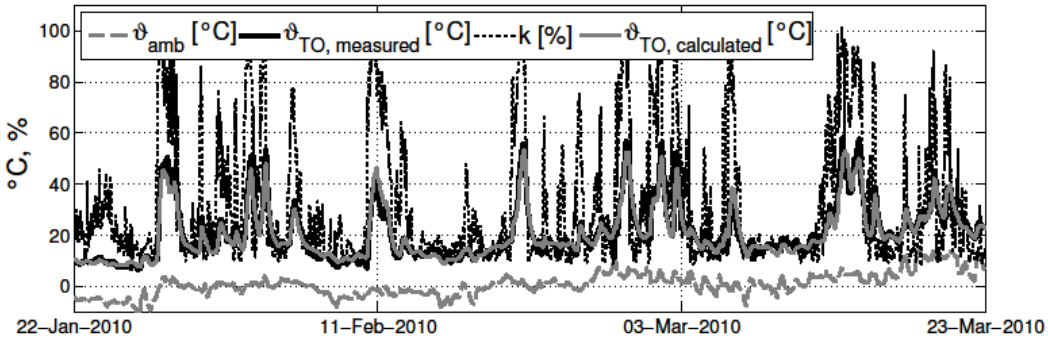

(b) Empirical evaluation time of three months

Figure 4: Influence of the evaluation period on the results for a 40 MVA ONAF-transformer

All transformers show a significant overload potential of at least 20 % at ambient temperatures below 10 °C. Moreover, the results attest ONAN transformers higher overload capabilities compared to ONAF transformers. **Figure 6** shows the influence of the various parameters in equation (2). Each graph represents the derived results for a 31.5 MVA ONAN transformer with one altered parameter out of x, y, g_r, H and ϑ_{HS} in comparison to the previously applied factors. For example, it can be seen that an increase of the hot-spot factor from $H = 1.3$ to $H = 1.6$ results in a decrease of almost 15 % of the maximal loading rate k_{max} independent of the ambient temperature. An increase of g_r from $g_r = 20$ K to $g_r = 25$ K causes similar consequences. Hence, the displayed correlations underline that the presented approach strongly depends on the hot-spot temperature calculation.

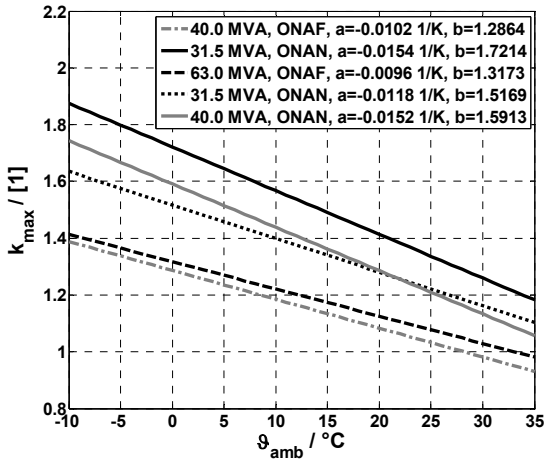

Figure 5: Maximum loading rate of the investigated transformers with $x = 0.8$, $y = 1.3$, $H = 1.3$, $g_r = 20$ K and $\vartheta_{HS} = 98$ °C

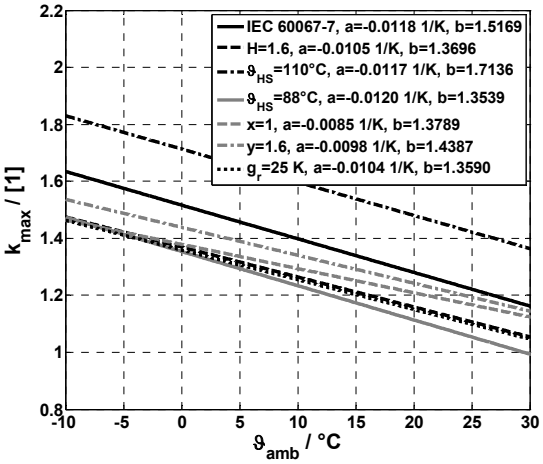

Figure 6: Maximum loading rate of a 31.5 MVA ONAN transformer

5 CONCLUSION

The assessment of overload capabilities of ONAN and ONAF transformers by means of thermal modelling offers network operators a profound insight into the correlation between the ambient temperature and the maximal applicable loading rate. However, the exact value of the maximal loading rate at a certain ambient temperature strongly depends on the calculation of the hot-spot temperature. Nevertheless, the provided certainty of the presented approach might be sufficient to allow network operators a responsible assessment of overloading potentials.

In reference to the illustrated results in Figure 5 and 6 it should be noted that IEC 60076-7 [1] explicitly limits the loading rate at standard operating conditions to $k_{max} = 1.3$. In addition, the presented results don't take the performance limits of attached accessories like the on-load tap-changer and bushings into account. For application of the introduced approach, also the specific condition concerning the service life (e. g. moisture content, DGA) of a certain transformer has to be regarded.

LITERATURE

[1] IEC 60076-7: Power Transformers Part 7: Loading guide for oil immersed power transformers, 2005

[2] S. Tenbohlen, M. Schäfer, H. Matthes: Beurteilung der Überlastbarkeit von Transformatoren mit online Monitoringsystemen, Elektrizitätswirtschaft, Jg. 99 (2000), H. 1-2, S. 1-5

[3] VDI, VDI-Heat Atlas, 10th edition, Berlin: Springer, 2006